

ORIGINAL RESEARCH

Open Access

Pilot protection of hybrid MMC DC grid based on active detection



Guobing Song, Junjie Hou^{*} , Bing Guo and Zhehong Chen

Abstract

Considering the advantages and limitations of traditional identification method, combined with the strategy of active detection, the principle of DC grid pilot protection based on active detection is proposed to improve the sensitivity and reliability of hybrid MMC DC grid protection, and to ensure the accurate identification of fault areas in DC grid. By using the DC fault ride-through control strategy of the hybrid sub-module MMC, the fault current at the converter station DC terminal is limited. Based on the high controllability of hybrid MMC, sinusoidal fault detection signals with the same frequency are injected into the line at each converter station. Based on model recognition, the capacitance model condition is satisfied by the detected signals at both ends during external faults whereas not satisfied during internal faults. The Spearman correlation coefficients is then introduced, and the correlation discriminant of capacitance model is constructed to realize fault area discrimination of DC grid. The simulation results show that the active detection protection scheme proposed in this paper can accurately identify the fault area of DC grid, and is not affected by fault impedance and has low sampling rate requirement.

Keywords: Hybrid MMC DC grid, Fault ride-through control strategy, Active detection, Model recognition, Pilot protection

1 Introduction

Nowadays most of flexible DC transmission projects use half-bridge submodules (HBSMs) based modular multi-level converter (MMC) which lacks DC fault clearance capability, and thus is suitable for cable schemes with low DC failure rates. However, due to the complexity of the transmission environment and the increase of distance and capacity, overhead lines are becoming increasingly popular for future flexible DC transmission projects [1–6]. For example, the Zhangbei 500 kV flexible DC transmission project uses half-bridge submodules based MMC with overhead transmission lines.

Overhead lines have a high probability of failure and the topology of the half-bridge converter requires a very short blocking time. After blocking, the DC power grid is isolated from the external power grid. The recovery and restart process of the DC power system is complicated, which makes power recovery time long. This may lead to the loss of stability of the connected AC system. In addition, the free-wheeling diodes in the MMC will also

form an uncontrolled rectifier bridge, resulting in large fault current feeding to the fault point. Considering that there is no natural zero crossing for DC current, DC circuit breakers have to create artificial current zero leading to complex circuitry and high cost. In the meantime, the relay protection must isolate the fault within milliseconds and requires high reliability and speed. Therefore, the development and application of half-bridge converter cooperated with DC circuit breaker need further study.

The full-bridge submodule has negative voltage output capability, and can directly block the converter to suppress the fault current. However, if converter blocking method is adopted, all the converters will have to be blocked after fault occurrence. During the blocking state, the DC power grid is isolated from the external power grid. The restart process of the DC grid is relatively complicated, resulting in a long power recovery time, which may cause the connected AC system to lose stability [7–9]. On the other hand, the high controllability of the full bridge submodules can be utilized to realize DC fault ride-through by controlling the number of the submodules switched in instead of blocking. This method can ensure the converter to continue providing reactive power support to the AC

* Correspondence: 826686025@qq.com

School of Electrical Engineering, Xi'an Jiaotong University, Xi'an 710049, China

side during DC faults. Compared with full-bridge MMC, hybrid MMC is composed of half-bridge and full-bridge submodules, which has certain economic advantages while ensuring DC fault clearance capability. DC overhead line transmission system based on hybrid MMC is now being considered as one of the future development trends [7–9], e.g. the DC project in Wudongde under construction.

At present, there is no mature protection scheme for flexible DC transmission line protection, and at this stage, guidance can only be provided from the traditional current source HVDC system. The protection are mainly divided into main protection and backup protection [10–16].

- 1) For the main protection, traveling wave protection and differential undervoltage protection are easily affected by fault impedance, noise, lightning, sampling rate, DC boundary, etc. Thus, the reliability of protection is low and the protection may have dead zones [10].
- 2) For the backup protection which is usually current differential protection, when the line is long, the delay introduced due to transmission delay, transient process and other factors, becomes too long for the flexible DC transmission system. For this reason, many researchers have proposed various new pilot protection principles for DC lines [11–15]. However, most of them depend on the DC boundary and the polarity characteristics of fault component in the initial transient of the fault. The pilot protection based on traditional model identification realizes fault identification by identifying the equivalent topology model of the line and has higher reliability [16]. However, the protection performance is closely related to the effective fault information extracted and line parameters, whereas the differential term of electrical quantity is easily affected by the initial instantaneous harmonic factor of the fault [17], and thus, the protection performance needs to be further improved.

In addition, considering that the flexible DC system has extremely short blocking time, the protection principle based on effective fault information will be limited. The reliability and sensitivity of the above protection principles will be affected. Therefore, it is urgent to study the protection principle of new DC power grid.

Based on the high controllability of hybrid MMC converter, active detection, protection and reclosing technology is becoming a new research hotspot. Researchers in [18, 19] use square wave injection method to achieve fault detection according to traveling wave transmission theory. However, the influence of fault impedance and sampling

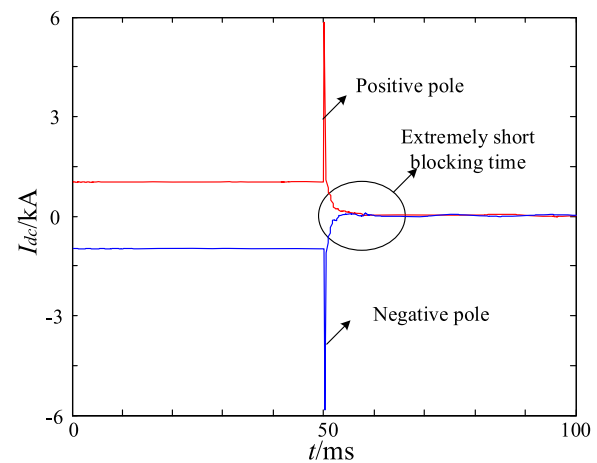


Fig. 1 Fault blocking of full bridge MMC system

rate on traveling wave may affect the results of fault discrimination. When applied to line protection, there still exists a problem of protection dead zone. In [20, 21], it points out that under coordinated control and protection, since the DC current is always under control, the converter will not be blocked due to overcurrent, and the DC system no longer has to detect and identify the fault line within milliseconds after fault occurrence. This makes it possible for the DC protection to use some advanced algorithms to improve the accuracy of fault detection and identification. The above researches provide good references for converter control and protection integration.

Based on the above analysis, this paper proposes a pilot protection of hybrid MMC DC grid based on active detection. The proposed protection makes full use of the high controllability of the hybrid MMC system, combined with the strategy of fault ride-through and active detection. Considering identification method, the Spearman correlation coefficient is introduced to construct the correlation discriminant of the capacitance model, in which the capacitance model condition satisfied by the detected signals at both ends for external faults while not satisfied for internal faults. The proposed protection is not easily affected by the initial instantaneous harmonic factor of the fault. Compared with traditional differential current protection, the proposed protection method is faster and won't be affected by distributed capacitance. The principle of DC grid pilot protection based on active detection is proposed and is verified by theoretical analysis and simulation.

2 Realization of active injection for protection

2.1 Significance of active detection protection

When traditional identification method is applied to DC power grid, it will be affected by the limitation of effective fault information, frequency-dependent parameters of the lines and other factors.

2.1.1 Effect of reliability

The fast rise of fault current in flexible DC system and the poor capability of power electronic equipment to withstand overcurrent mean converters have to be blocked very quickly. For a full-bridge MMC DC system, the time from blocking of converter to attenuation of fault current to zero is less than 10 ms [1], and therefore, the fault characteristics are not significant. An example of the fault DC currents is shown in Fig. 1 where the fault occurs at time of 50 ms.

2.1.2 Effect of sensitivity

Real transmission line parameters are frequency-dependent, and the frequency band of fault information is wide after DC line faults. Figure 2 illustrates an example of an external fault when applying the traditional model identification method under a wide frequency band.

There are differences among line parameters under different frequencies. The traditional identification method uses the electrical quantity information at the initial moment of the fault to identify the fault. The frequency information of the electrical quantity at the initial moment of the fault is complex, while the line parameters are frequency-dependent, so these parameters are different:

$$i_m(t) \neq C(\omega) \frac{du_m(t)}{dt}, i_n(t) \neq C(\omega) \frac{du_n(t)}{dt} \quad (1)$$

where $C(\omega)$ is the capacitance value at a specific frequency.

According to (1), the parameters corresponding to different frequencies are different, so the accuracy of model identification will be reduced in principle and the protection performance based on model identification will be affected.

In addition, considering that the protection principle based on model identification method is closely related to the numerical calculation of the first-order differential term, the common method is to replace the differential value with the difference between two sampling points as

$$\frac{u(n) - u(n-1)}{Ts} = k \frac{du(t)}{dt} \quad (2)$$

where Ts is the sampling interval.

It can be seen from (2) that since the converter is blocked quickly, when the information at the initial moment of the fault is used, the frequency content of the fault information is complex, and k in (2) will become a time-varying parameter [17]. Thus, the accuracy of model identification will be reduced.

2.2 Proposed methodology

In view of the limitations of traditional model identification pilot protection principle applied to DC power grid, this paper proposes an active detection pilot protection scheme based on the high controllability of the converter. Taking the two-terminal system as an example, its MMC active control strategy and the fault models at the specific frequency for internal and external faults are shown in Fig. 3.

2.2.1 Reliability

By injecting controllable sinusoidal signals with certain amplitude, frequency, injecting time and duration, the fault model can be identified using the sinusoidal signals at that frequency (as shown in Figs. 3(a) and (b)) and the fault section of the DC line can be identified more precisely. Compared with the traditional model identification pilot protection principle, it can better obtain effective fault information and identify fault section.

2.2.2 Sensitivity

Considering the influence of frequency-dependent parameters of the lines, by injecting single frequency sinusoidal detection signals at both ends of the lines, the voltage and current ($u_{(m,n)}(\omega)$, $i_{(m,n)}(\omega)$) at the specific frequency are extracted from the positions where protections are installed for fault identification, as shown in Fig. 3(a) as:

$$i_{m(\omega)} = c(\omega) \frac{du_{m(\omega)}}{dt}, i_{n(\omega)} = c(\omega) \frac{du_{n(\omega)}}{dt} \quad (3)$$

$C(\omega)$ in the capacitance model can be determined, so the accuracy of fault model identification is improved in principle, and the influence of frequency-dependent parameters of the lines is overcome.

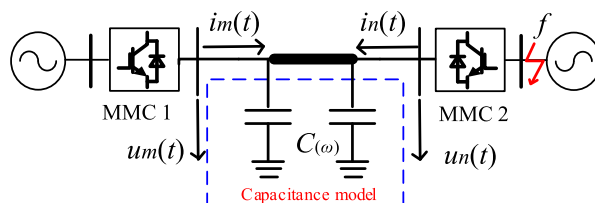


Fig. 2 Traditional model identification method

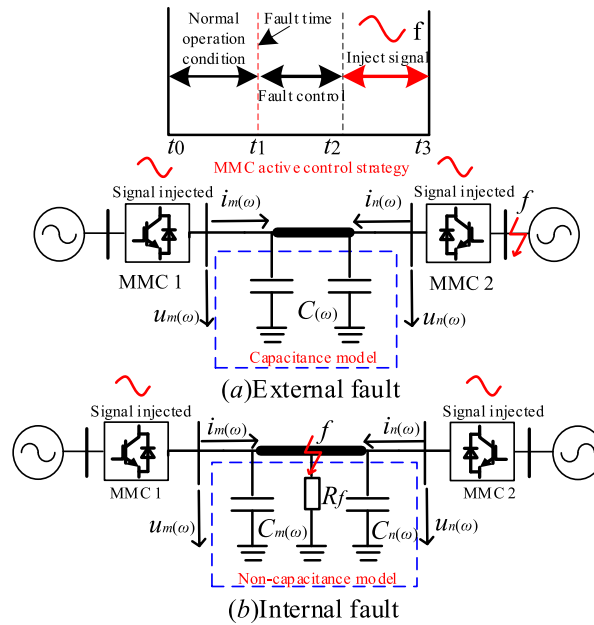


Fig. 3 Block diagram of active pilot protection

In addition, the frequency of the characteristic signal is determined considering the sinusoidal signal injected as

$$u_{(\omega)} = A \sin(\omega t + \phi) \tag{4}$$

When the difference between two sampling values is used instead of the differential value, there is:

$$\begin{aligned} \frac{u_{(\omega)}(n) - u_{(\omega)}(n-1)}{T_s} &= k \frac{du_{(\omega)}}{dt} \\ &= \frac{2}{\omega T_s} \sin(\omega T_s/2) \frac{du_{(\omega)}}{dt} \end{aligned} \tag{5}$$

From (5), the difference between the two sampling values and the differential value are correlated by the coefficient $2/(\omega T_s)\sin(\omega T_s/2)$, which is independent of t and the initial phase angle ϕ , and is only related to ω and T_s . Therefore, the coefficient is constant and error correction can be performed.

Compared with the traditional model identification pilot protection using initial fault transient information, the method proposed in this paper overcomes the influence of frequency-dependent parameters and error factors of electrical quantity differential terms [17], and thus improves the sensitivity of the protection. The injecting time, amplitude, length and type of detection signal are controllable, leading to higher reliability in principle.

Thus, taking full consideration of the above factors and combined with the high controllability of MMC and the advantages of traditional identification method, the

principle of DC grid pilot protection based on active detection is proposed in this paper.

3 Injection strategy of active detection

3.1 Fault ride-through strategy of hybrid MMC

For hybrid MMC, the control strategy adopts closed-loop controls similar to those of the half-bridge MMC and is shown in Fig. 4. As seen, the outer loop bridge arm voltage control regulates the average capacitor voltage of the bridge arm submodules, and the voltage balance algorithm is adopted to switch in or out the submodules based on the set upper and lower limits of the allowed fluctuation of the capacitor voltage [4, 7, 8]. When the mixing ratio of the full-bridge and half-bridge submodules of the bridge arm reaches 1:1, the range of the DC voltage modulation ratio M_{dc} of the hybrid MMC is $[-0.1, 1]$, and the output range of the bridge arm voltage is $[-0.1, 1]$ times the rated DC voltage under unit power factor condition [4, 7, 8].

As can be seen from Fig. 4, the control strategy of the hybrid MMC is different from the traditional half-bridge MMC with an added closed-loop DC control loop. The DC current reference value I_{dcref} generated by the outer DC voltage control loop is taken as the input of the inner DC current control loop, and the DC voltage reference value is obtained through the PI regulator to act on the switching process of the submodules to realize the control of DC voltage and current.

When the MMC system detects that the DC voltage drops to 0.5p.u or the DC current rises to 2p.u, it switches to the fault control mode 1, and sets the DC current reference I_{dcref} of the inner loop to a pre-set value I_{dcset} , thereby controlling the DC current to the

sub-modules in practical engineering is around 10 kHz, and the sampling rate of electrical parameters in engineering protection installation is normally lower than 20 kHz [2–7].

- 2) Considering the attenuation effect of transmission lines on electric quantities, it is appropriate to select low frequency band. As an example, the quantities transmission attenuation curve of typical overhead lines are illustrated in Fig. 6.

As can be seen from Fig. 6(a), as the length of the line and frequency increase, the amplitude attenuation becomes more severe. While from Fig. 6(b), it can be seen that the attenuation of the signal information amplitude at a frequency of 200 Hz or higher becomes more and more significant. Therefore, the characteristic frequency of the signal should be lower than 200 Hz.

- 3) The influence of distributed capacitance current can be further reduced with the reduction of filter cut-off frequency [22], and the cutoff frequency can be approximated according to the fitting error of linear voltage distribution as:

$$E_m = 1 - \cos(\omega l / 2v) \tag{9}$$

where ω is the cut-off frequency of the low-pass filter, l is the line length, and v is the wave velocity.

Taking a typical length of 250 km as an example and considering that the wave velocity is approximately the velocity of light, if the cut-off frequency of the low-pass filter is 100 Hz, the fitting error E_m is calculated as 4.9% which is within the acceptable range [22]. The lower the cut-off frequency is, the smaller the fitting error and the influence by the distributed capacitance current are.

Considering the above factors, the frequency of the injected signal is selected to be 100 Hz.

3.3.2 Length of injected signal

In order to ensure the reliability of protection principle, the length of injected signal should not be too short so as to provide sufficient margin for arc extinguishing time and reclosing discrimination time [18, 19]. On the other hand, the length should not be too long to ensure the speed of protection. Considering the delay time of the characteristic signal transmitted to the fault point or reflected back from the opposite end system, the maximum delay is about 2 ms for the line length of the existing projects not exceeding 300 km. In addition, the total data length should be greater than the data transmission delay length. Based on the above factors, the length of the injected characteristic frequency signal in each converter station is chosen to be 5 ms.

3.3.3 Amplitude of injected signal

Taking account of the tolerance of power electronic equipment at the protection installation point and the converter, the amplitude of the characteristic signal should not be too large, while be sufficient to reduce the influence of line frequency attenuation characteristics to facilitate model identification and analysis. Considering the tolerance of MMC to short circuit current is limited to 2~3 times of rated current, according to [18, 19], it is suggested that the amplitude of active square wave pulse should not exceed 0.2 times of the rated DC line voltage. Therefore, 0.1 times the rated voltage is chosen as the injection amplitude of the sine wave detection signal.

4 Scheme of the pilot protection for DC grid based on active detection

4.1 Identification method

According to the high controllability of the hybrid MMC converter, the DC current at each end of the DC system is controlled, and the DC current I_{dcref} of the inner loop is set to I_{dcset} (0.1p.u) under fault conditions. When it is detected that the current is limited to the range by the converters, the system will switch to the fault control 2 mode,

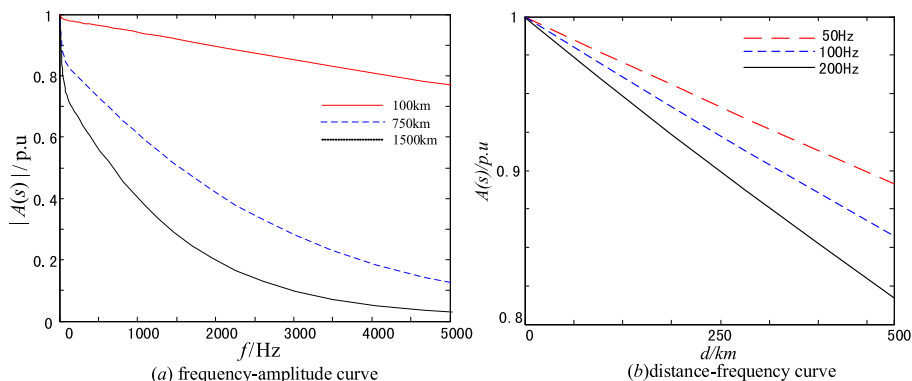


Fig. 6 Attenuation curve of signal propagation

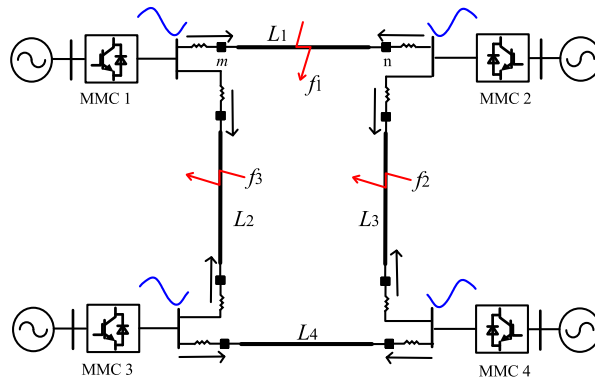


Fig. 7 Four-terminal hybrid MMC DC grid

and set the DC voltage reference value U_{dcref} to U_{dcset} , i.e. injecting sinusoidal voltage characteristic signals with equal frequency into each end at the same time.

Taking a four-terminal grid as an example shown in Fig. 7, combined with the principle of frequency selection in Section 3.3, the characteristic frequency voltage of 100 Hz is injected separately, and the voltage and current information at the characteristic frequency are extracted at the relay protection installations.

Taking the single-pole fault of DC line L_1 and DC line L_2 as examples, the protection installation positions m and n on DC line L_1 are selected for analysis.

When DC line L_1 fails, the equivalent circuit diagram is shown in Fig. 8, where i_m , i_n , and u_m , u_n are the respective current and voltage values at the characteristic frequency measured after characteristic signal injection. I_{cm} and I_{cn} are the equivalent capacitance currents flowing through the two-terminal lines at the characteristic frequency, respectively. Z_{lm} , Z_{ln} , and C_{lm} , C_{ln} are the impedance and capacitance values on both sides of the DC line at the characteristic frequency, respectively, and R_f represents the fault impedance.

As can be seen from Fig. 8, when the DC line L_1 fails, the capacitance currents i_{cm} and i_{cn} flowing through the capacitances at both ends of the DC line can be expressed as:

$$\begin{cases} i_{cm} = C_{lm} \frac{du_m}{dt} \\ i_{cn} = C_{ln} \frac{du_n}{dt} \end{cases} \quad (10)$$

The fault current injected into the fault point by the DC system from both sides is:

$$i_m + i_n = i_{cm} + i_{cn} + i_f \quad (11)$$

where i_f is the short-circuit current flowing through the fault point.

The differential current i_{cd} and voltage u_{cd} are defined as:

$$i_{cd} = i_m + i_n, u_{cd} = u_m + u_n \quad (12)$$

From (10)~(12), the differential voltage and current at both ends of the line have the following relationship:

$$i_{cd} = C_{lm} \frac{du_{cd}}{dt} + (C_{lm} = C_{ln}) \frac{du_m}{dt} + i_f \quad (13)$$

It can be seen from (13) that there is no linear relationship between differential voltage u_{cd} and current i_{cd} across the DC line due to the existence of the last two terms when the DC line has an internal fault. Therefore, the defined differential voltage and current do not satisfy the capacitance model.

When the DC line L_2 fails, it is an external fault for the protection installation point m and n at both ends of L_1 , as shown in Fig. 9.

As can be seen from Fig. 9, the capacitance currents i_{cm} and i_{cn} flowing through the capacitances at both ends of the DC line L_1 can be expressed as:

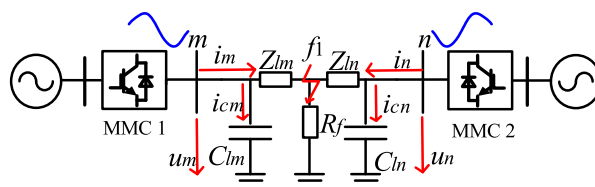


Fig. 8 Internal fault equivalent diagram

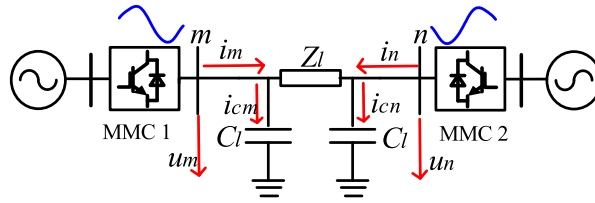


Fig. 9 External fault equivalent diagram

$$\begin{cases} i_{cm} = C_l \frac{du_m}{dt} \\ i_{cn} = C_l \frac{du_n}{dt} \end{cases} \quad (14)$$

The fault current injected into the fault point by the DC system at both ends is:

$$i_m + i_n = i_{cm} + i_{cn} \quad (15)$$

According to (14) and (15), differential current i_{cd} and voltage u_{cd} satisfy:

$$i_{cd} = C_l \frac{du_{cd}}{dt} \quad (16)$$

It can be seen from (16) that there is linear relationship between differential voltage u_{cd} and current i_{cd} . Therefore, the defined differential voltage and current satisfy the capacitance model.

Considering the compensation effect when faults occur, the differential voltage in (16) shall be compensated as follows:

$$\begin{cases} \frac{du'_{cd}}{dt} = \frac{d(u_{cd} + K_c u_0)}{dt} \\ K_c = \frac{\sqrt{2}}{2} (C_0/C_1 - 1) \end{cases} \quad (17)$$

where u'_{cd} represents the compensated differential voltage of each phase, and u_0 represents the zero-mode voltage at the protection installation positions on both sides. K_c represents the zero-mode compensation coefficient, and C_0 and C_1 represent the zero-mode and line-mode capacitances of the unit length of the line, respectively.

4.2 Introduction of line model correlation discrimination

According to Section 4.1, the defined differential voltage and current satisfy the capacitance model when the external fault occurs. The differential current i_{cd} increases with the increase of the differential voltage derivative du_{cd}/dt as can be seen in (16), indicating a positive correlation. When the internal fault occurs, the capacitance model is not satisfied and the differential current i_{cd} has no direct relationship with du_{cd}/dt .

Based on the above characteristics, this paper introduces the Spearman correlation coefficient [23] to measure the correlation between the two variables by checking whether

they have synchronous change trend (increasing or decreasing at the same time). Compared with Pearson correlation coefficient [24], Spearman correlation coefficient is not affected by data dimension, which makes correlation coefficient insensitive to large abnormal numbers and is more suitable for processing discrete data. Therefore, Spearman correlation coefficient is selected as the measurement method of similarity for model identification based on active detection.

The Spearman correlation coefficient is calculated by product moment and the correlation between two variables (y and z) is expressed by multiplying the deviation between them based on the deviation between the two variables and their respective average values as

$$r(y, z) = \frac{\sum_{i=1}^n (y(i) - \bar{y})(z(i) - \bar{z})}{\sqrt{\sum_{i=1}^n (y(i) - \bar{y})^2 \sum_{i=1}^n (z(i) - \bar{z})^2}} \quad (18)$$

where $r(y, z)$ is the correlation coefficient, and the value range is $[-1, +1]$. i is the sampling point, T_s the sampling interval and N the total number of sampling points of the data.

$r < 0$ means negative correlation and the increase of one variable may cause the decrease of the other variable, whereas $r = 0$ means no correlation between the two groups of variables and the two groups of variables are largely independent. When $r > 0$, the positive correlation is satisfied, and the increase of one variable may cause the increase of the other. For $0 < r < 0.5$, there is weak positive correlation, while $0.5 \leq r < 1$ indicates strong positive correlation and $r = 1$ indicates perfect positive correlation.

4.3 Fault identification

According to Section 3.1 and 3.2, combined with active detection strategy and correlation discrimination principle of DC line model, voltage and current differential values in the fault model do not have positive correlation characteristics for internal faults, while for external faults, positive correlation characteristics are satisfied. This can be used to construct protection criteria. Replacing the differential form by the difference form, the instantaneous values of

differential current and voltage derivatives at the i -th sampling point $y(i)$ and $z(i)$ can be expressed as:

$$\begin{cases} y(i) = i_{cd}(i) \\ z(i) = \frac{\omega T_s}{2 \sin(\omega T_s/2)} \frac{u_{cd}(i) - u_{cd}(i-1)}{T_s} \end{cases} \quad (19)$$

where T_s is the sampling interval, ω represents the angular frequency of the characteristic signal, $\omega = 2\pi f$ and $f = 100$ Hz.

For convenience, replacing the right side of $z(i)$ in (19) with $u_{cd}(i)'$ as.

$$u_{cd}(i)' = \frac{\omega T_s}{2 \sin(\omega T_s/2)} \frac{u_{cd}(i) - u_{cd}(i-1)}{T_s} \quad (20)$$

Substituting (19) and (20) into (18), the capacitance model correlation discrimination equation is constructed as:

$$r(y, z) = \frac{\sum_{i=1}^N (i_{cd}(i) - \overline{i_{cd}}) (u_{cd}(i)' - \overline{u_{cd}(i)'})}{\sqrt{\sum_{i=1}^N (i_{cd}(i) - \overline{i_{cd}})^2 \sum_{i=1}^N (u_{cd}(i)' - \overline{u_{cd}(i)'})^2}} \quad (21)$$

According to the correlation discriminant of the fault model in (21), the fault section of the DC power grid is discriminated.

By comparing the set value of positive correlation coefficient, the correlation can be used to further determine the fault section of DC power grid. Then the operating criterion is as follows:

$$r(y, z) < r_{set} \quad (22)$$

where r_{set} is the set value of positive correlation coefficient.

When $r(w(i), x(i)) < r_{set}$, positive correlation is not satisfied, which indicates an internal fault. In contrast, when $r(w(i), x(i)) > r_{set}$, positive correlation is satisfied, indicating an external fault. In order to improve the reliability while considering the sensitivity, the set value should theoretically be as large as possible, with the maximum value being 1. However, considering the influence caused by data acquisition, a certain margin should be reserved with strong positive correlation still satisfied, so the threshold value is set to 0.5.

The fault identification process is thus as follows.

- The two correlation coefficients at the protection installation on both sides of the positive and negative poles are calculated respectively;
- If the two correlation coefficients are all greater than 0.5, it means external faults;
- If at least one of the two correlation coefficients is less than 0.5, it means internal faults, and the

correlation coefficient less than 0.5 corresponds to the faulty pole.

5 Process of protection

The process of pilot protection of hybrid MMC DC grid based on active detection when a DC line fails is given as follows and the flow chart is shown in Fig. 10.

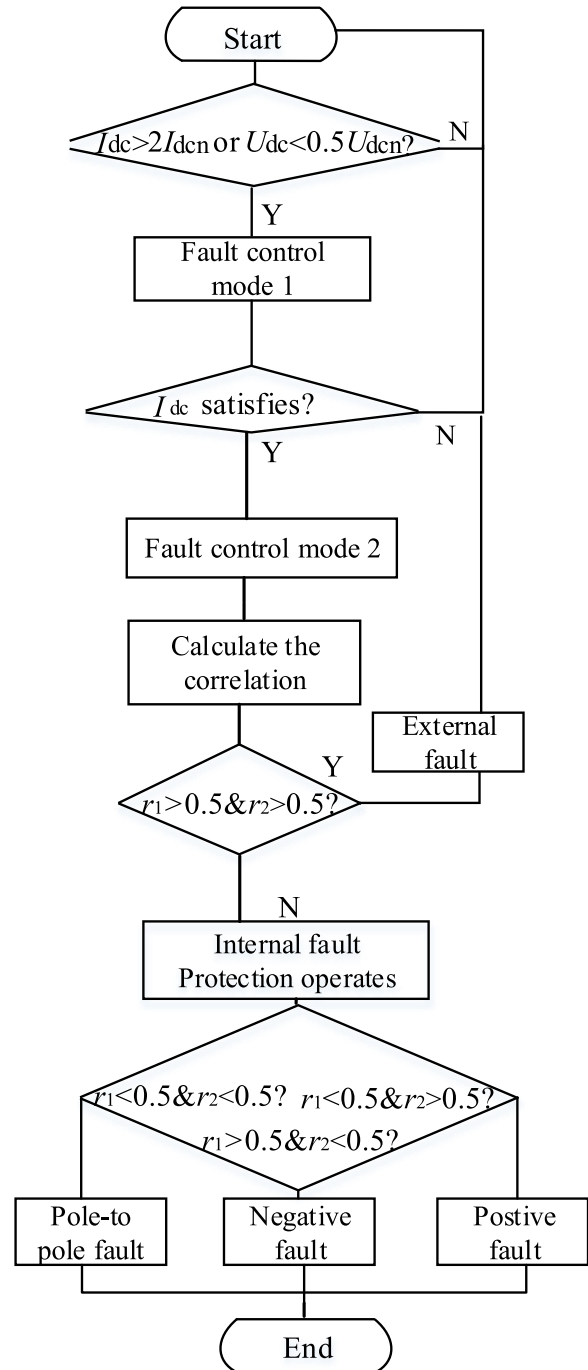


Fig. 10 Protection flow chart

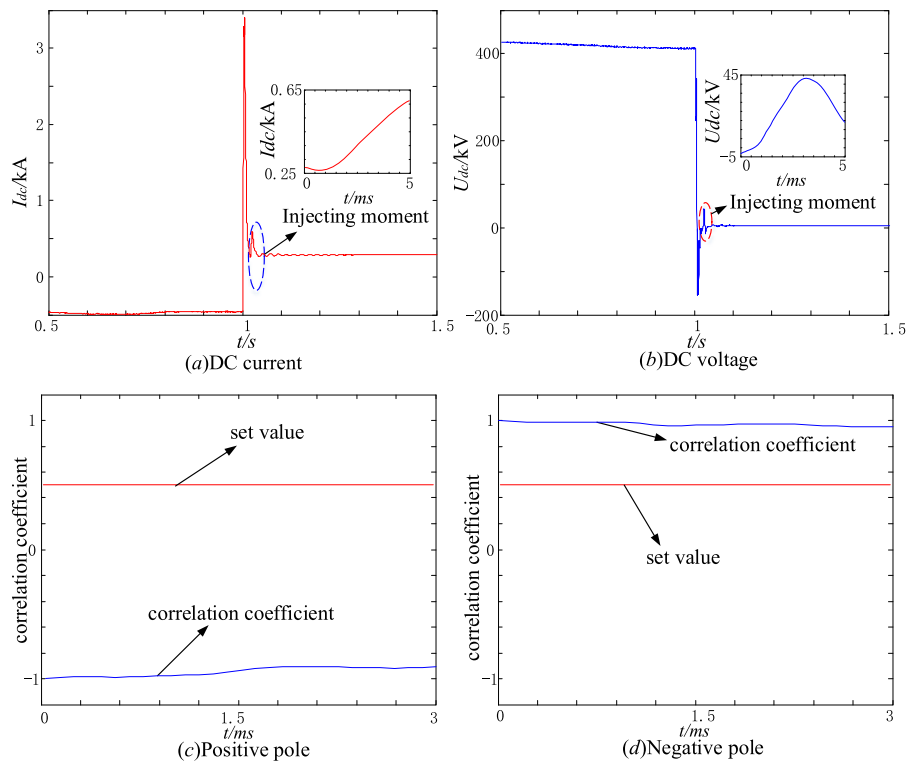


Fig. 11 f_1 point pole-to-ground fault

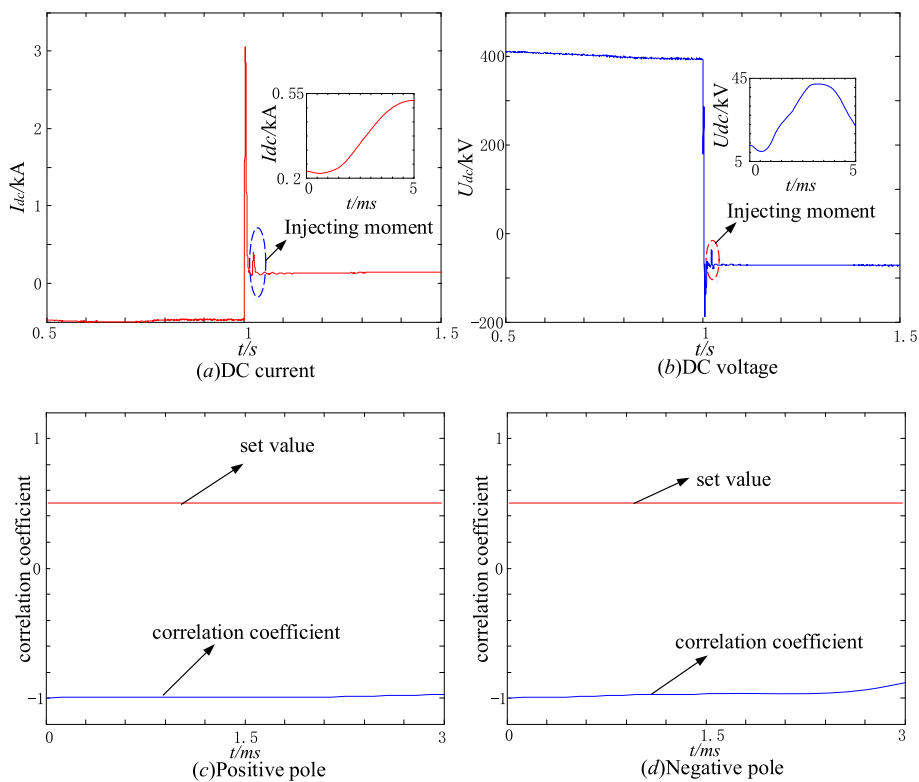


Fig. 12 f_1 point pole-to-pole fault

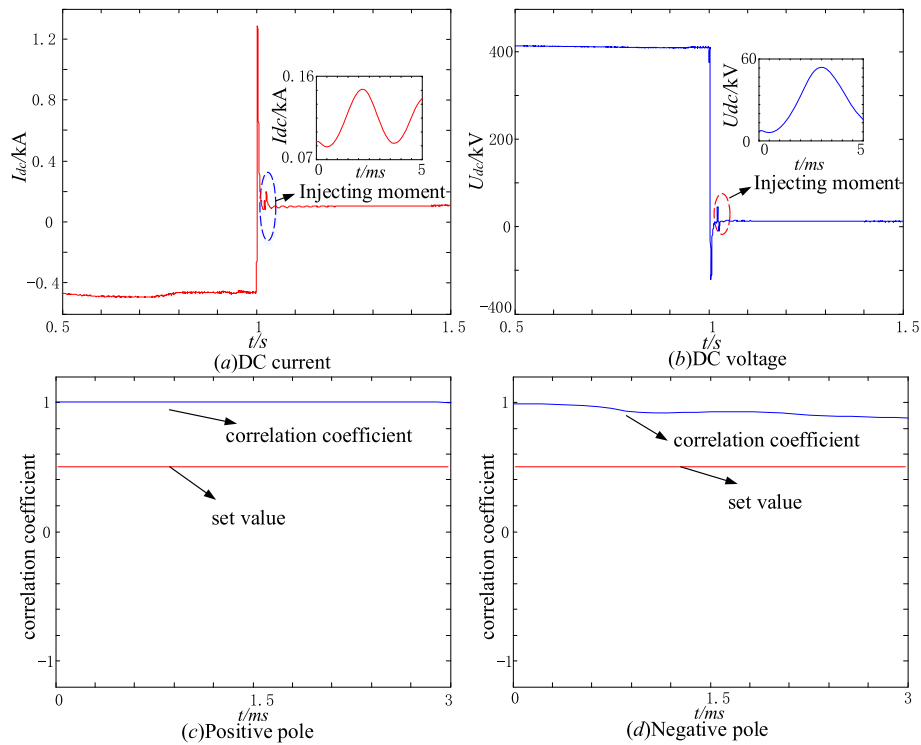


Fig. 13 f_2 point fault

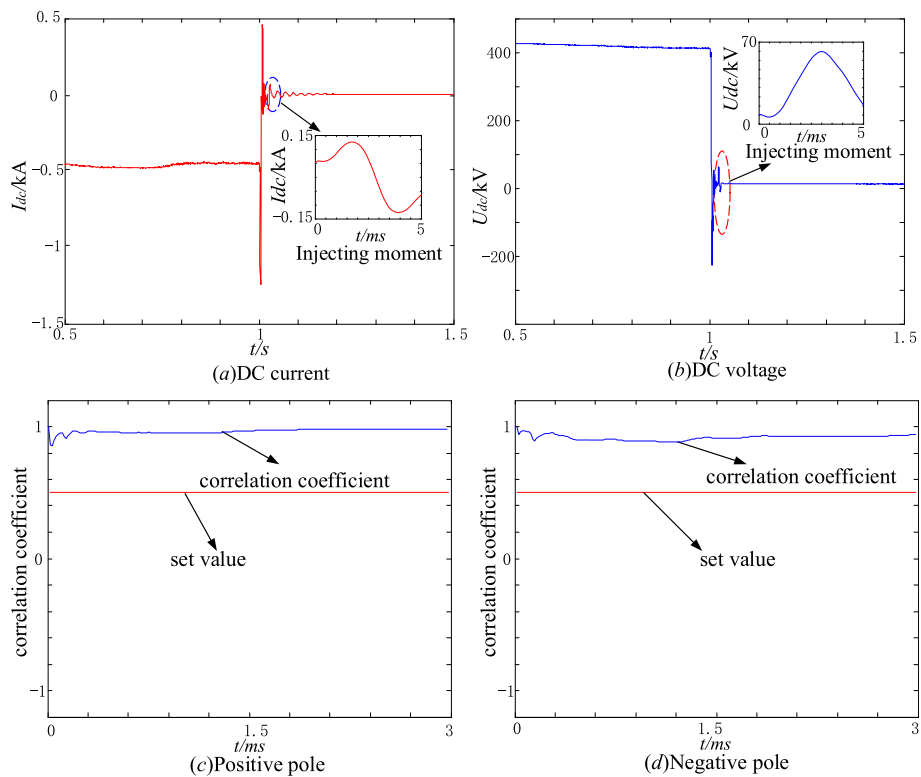


Fig. 14 f_3 point fault

Table 1 Protection results

Fault position	Correlation coefficient (Positive/Negative)	Fault section	Fault pole	Operate or not(Y/N)
f_1 (pole-to-ground)	- 0.881/0.934	internal	pole-to-ground	Y
f_1 (pole-to-pole)	-0.872/- 0.921	internal	pole-to-pole	Y
f_2 (pole-to-pole)	0.976/0.963	external	/	N
f_3 (pole-to-pole)	0.977/0.954	external	/	N

- 1) When the hybrid MMC system detects that the DC voltage drops to 0.5p.u or the DC current rises to 2p.u, it switches to the fault control mode 1 to limit the fault current to a pre-set value. The converter stations at both ends are not blocked during the fault but remain continuous control.
- 2) In order to ensure the speed and reliability of fault location, when it detects that the fault current is within the set value range I_{dcset1} (all three consecutive sampling points are satisfied), the fault control mode 1 is switched to the fault mode 2. Taking the four-terminal grid as an example in this paper, sinusoidal voltage waves of 100 Hz, with amplitude of 0.1p.u, initial phase of 0, and length of 5 ms, are injected respectively by the four converters.
- 3) The 100 Hz characteristic frequency electrical quantity information is extracted from the protection installation positions of the positive and negative lines, and is fed into (21). Through calculating the correlation coefficients r_1 and r_2 of the positive and negative lines and comparing with the set values, accurate discrimination of the fault area is realized, and corresponding protection operates.

6 Results and discussion

Referring to the hybrid MMC HVDC transmission system and actual parameters, a ± 400 kV bipolar four-terminal hybrid MMC DC grid as shown in Fig. 7, is

simulated in PSCAD, with the rated capacity of 1200 MVA. The 250 km long DC line is simulated using frequency dependent line model. The aerial mode and zero mode impedance are $0.027 + j0.87 \Omega/\text{km}$ and $0.046 + j1.97 \Omega/\text{km}$, respectively at 100 Hz frequency. Each bridge arm consists of 200 sub-modules with equal numbers of half-bridge and full-bridge sub-modules, and an arm reactance of 19 mH. Capacitance of each sub-module is 15mF. The AC system is rated at 380 kV with the equivalent short circuit impedance of 18%. Simulation time step is selected to be 100 μs , the sampling frequency for signal processing is 10 kHz and the simulation duration is 2 s. The fault occurs at 1 s.

The fault locations are respectively at f_1 (pole-to-pole fault/ pole-to-ground fault in the midpoint of DC line L_1), f_2 and f_3 (pole-to-pole fault in the midpoint of L_2 and L_3 , which are external faults for L_1), lasting for 1 s. The simulation data obtained by PSCAD are imported into MATLAB to verify the protection algorithm. In order to improve the accuracy of the algorithm, considering the data transmission delay, the protection algorithm can use the last 3 ms of the total data length (5 ms) for operation.

6.1 Verification of protection scheme

When the DC line fails, the systems on both sides are switched to fault control mode 1, and the DC current reference value is set to 0.1p.u. When the fault current is detected to have decreased to 0.1p.u at m (with three

Table 2 Protection results under noise interference

Distance km / (fault type)	Correlation coefficient (positive/negative)	Fault section	Fault pole	Operate or not (Y/N)
30(single-pole)	-0.873/0.945	internal	positive	Y
100(single-pole)	-0.923/0.937	internal	positive	Y
150(single-pole)	-0.895/0.916	internal	positive	Y
250(single-pole)	-0.832/0.907	internal	positive	Y
f_2 (pole-to-pole)	0.941/0.932	external	/	N
30(pole-to-pole)	-0.824/-0.865	internal	pole-to-pole	Y
100(pole-to-pole)	-0.866/- 0.897	internal	pole-to-pole	Y
150(pole-to-pole)	-0.813/- 0.821	internal	pole-to-pole	Y
250(pole-to-pole)	-0.842/- 0.851	internal	pole-to-pole	Y
f_3 (pole-to-pole)	0.913/0.922	external	/	N

From the simulation results, it can be seen that the protection principle has strong anti-interference capability

Table 3 Protection results under grounding fault with fault impedance

Fault impedance Ω /distance	Correlation coefficient (positive/negative)	Fault section	Fault pole	Operate or not (Y/N)
0.01/150	-0.903/0.931	internal	positive	Y
50/150	-0.801/0.928	internal	positive	Y
100/150	-0.731/0.916	internal	positive	Y
300/150	-0.633/0.902			
0.01/250	-0.923/0.919	internal	positive	Y
50/250	-0.836/0.917	internal	positive	Y
100/250	-0.766/0.913	internal	positive	Y
300/250	-0/612/0.901			
0.01/ f_2	0.942/0.918	external	/	N
50/ f_2	0.937/0.922	external	/	N
100/ f_2	0.926/0.911	external	/	N
0.01/ f_3	0.954/0.947	external	/	N
50/ f_3	0.946/0.932	external	/	N
100/ f_3	0.928/0.915	external	/	N

From the simulation results, it can be seen that the model identification pilot protection based on active detection using the capacitance model to identify the fault section has strong anti-fault impedance capability in principle

continuous sampling points), the converter is switched to fault control mode 2. The 100 Hz sine wave signal is injected into the line by changing the DC voltage reference value, and the correlation coefficients of positive and negative poles is calculated by using (22). Take L1 as an example, the positive DC current, DC voltage and the correlation results at m when an pole-to-pole fault occurs are shown in Fig. 11, Fig. 12, Fig. 13, Fig. 14. The correlation coefficients in Fig. 11, Fig. 12, Fig. 13, Fig. 14. are averaged, and the results are summarized in Table 1.

From Fig. 11, Fig. 12, Fig. 13, Fig. 14. it can be concluded that when the system switches to the fault control mode 1 after fault occurrence, the fault current can be limited to the set value within a few milliseconds. Then the system switches to fault control mode 2. By changing the reference value of DC voltage and injecting signals into the line, it can be seen that DC voltage and current are approximate sine waves within one cycle. In case of internal pole-to-pole fault, the correlation coefficient of the positive and negative poles is less than the set value, thus the protection can operate correctly. When an external fault occurs, the correlation coefficient of the positive and negative poles is

larger than the set value, and the protection does not operate.

6.2 Anti-interference capability

Considering the interference of external noise and transformer transmission error on the protection principle in practical engineering, this paper uses random Gaussian white noise to verify the anti-interference performance of the principle. The signal-to-noise ratio of the white noise signal is 30 dB. The anti-interference performance of internal metallic grounding fault and pole-to-pole fault in different fault positions (30 km, 100 km, 150 km, 250 km) of the DC line, and external pole-to-pole faults (f_2 and f_3) are verified as shown in Table 2.

6.3 Anti-fault impedance capability

Taking internal faults with 0.01 Ω , 50 Ω , 100 Ω fault impedances at 150 km and 250 km of f_1 in the positive pole and external faults at the midpoint of f_2 and f_3 as examples, the anti-fault impedance performance of the principle is tested, as shown in Table 3. In addition, in

Table 4 Protection results with different sampling rates

Sampling rates (kHz)	Correlation coefficient (positive/negative)	Fault section	Fault pole	Operate or not (Y/N)
2	-0.833/0.905	internal	positive	Y
5	-0.825/0.917	internal	positive	Y
10	-0.819/0.913	internal	positive	Y
15	-0.896/0.924	internal	positive	Y
20	-0.931/0.911	internal	positive	Y

From the simulation results, it can be seen that the correlation coefficient is largely not affected by the sampling rate, ensuring the correct operation of the protection in case of internal faults

Table 5 Protection results with different correlation coefficients

Methods	Correlation coefficient (positive/negative)	Fault section	Fault pole	Operate or not (Y/N)
Spearman	0.941/0.932	external	pole-to-pole	N
Pearson	0.618/0.594	external	pole-to-pole	N

From the simulation results, it can be seen that the Spearman correlation coefficient is more superior

order to verify the protection performance under internal fault with 300 Ω fault impedance, the trigger criterion of converter fault control is adjusted to that the DC voltage drops to 0.8p.u. or the DC current rises to 1.5p.u.

6.4 Performance at different sampling rates

Taking internal faults with 0.01 Ω transition impedance at 200 km in positive pole as an example, the protection scheme is tested with sampling rates of 2 kHz, 5 kHz, 10 kHz, 15 kHz and 20 kHz, as shown in Table 4.

6.5 Compared with Pearson correlation coefficient

Taking external pole-to-pole faults (f_2) as an example, the protection scheme is tested with sampling rates of 10 kHz, as shown in Table 5.

7 Conclusion

Combing the high controllability of hybrid MMC system, fault ride-through strategy and characteristic signal injection strategy, a pilot protection principle based on active detection is proposed in this paper using model identification. The following conclusions are obtained.

- 1) For the hybrid MMC converter system, its high controllability can be fully utilized, and the characteristic frequency signal can be injected by controlling the DC voltage through acting on the switching process of sub-modules to realize the control of DC current and voltage.
- 2) Characteristic signals of the same frequency can be injected into the lines at different converter stations, and the frequency characteristic signals extracted at the protection installation position. By utilizing the characteristic that the frequency signals satisfy the capacitance model for external faults but do not satisfy for internal faults, the fault section identification can be realized by combining the model identification method and the Spearman correlation identification method.
- 3) Pilot protection of hybrid MMC DC grid based on active detection is not affected by distributed capacitance current and is superior to traditional model identification protection principle in reliability and sensitivity. Combining the fault ride-through strategy and the active detection signal injection strategy, the proposed method is not affected by line frequency-dependent parameters and

electric quantity differential term errors while on the other hand, fault information can be used effectively and flexibly to identify fault sections. In addition, the proposed method has strong anti-fault impedance and anti-interference capability, and does not depend on high sampling rate and DC boundary.

Acknowledgements

Not applicable.

Authors' contributions

GS as the first author, contributed significantly to analysis and research of the paper, JH as the corresponding author, contributed significantly to the research, writing and submission of the paper. BG and ZC also helped to improve the paper quality. All the authors read and approved the submitted manuscript.

Funding

This work is supported by The National Natural Science Foundation key project (U1766209).

Availability of data and materials

Not applicable.

Competing interests

The authors declare that they have no competing interests.

Received: 19 November 2019 Accepted: 6 January 2020

Published online: 17 February 2020

References

1. Xu, Z., et al. (2016). *Flexible DC transmission system [M]*. Beijing: China Machine Press.
2. Xu, Z., Xue, Y., & Zhang, Z. (2014). VSC-HVDC technology suitable for bulk power overhead line transmission. *Proceedings of the CSEE*, 34(29), 5051–5062.
3. Guo, X., Zhou, Y., Mei, N., et al. (2018). Research on the fault current characteristic and suppression strategy of Zhangbei project. *Proceedings of the CSEE*, 38(18), 5438–5446.
4. Lin, W., Jovic, D., Nguéfeu, S., & Saad, H. (2015). Full-bridge MMC converter optimal design to HVDC operational requirements. *IEEE Transactions on Power Delivery*, 31(3), 1342–1350.
5. Guo, Y., Zhou, Y., Xu, J., et al. (2017). Control strategies of DC ice-melting equipments for full-bridge modular multilevel converters. *Automation of Electric Power Systems*, 41(5), 106–113.
6. Li, S., Xiuli W, Tai L, et al.(2016). Optimal design for hybrid MMC and its DC fault ride-through strategy. *Proceedings of the CSEE*, 36(7).1849–1858.
7. Zhou, M., Xiang, W., Lin, W., et al. (2018). Active current limiting control to handle DC line fault of overhead DC grid. *Power System Technology*, 42(7), 2062–2072.
8. Xiang, W., Lin, W., Xu, L., & Wen, J. (2017). Enhanced independent pole control of hybrid MMC-HVDC system. *IEEE Transactions on Power Delivery*, 33(2), 861–872.
9. Zhang, J., Xiang, W., Lin, W., et al. (2017). DC fault protection of VSC-HVDC grid based on hybrid MMC and DC switch. *Electric Power Construction*, 38(8), 52–58.
10. Song, G., Gao, S., Cai, X., et al. (2012). Survey of relay protection technology for HVDC transmission lines. *Automation of Electric Power Systems*, 36(22), 123–129.

11. Dong, X., Tang, L., Shi, S., et al. (2018). Configuration scheme of transmission line protection for flexible HVDC grid. *Power System Technology*, 42(6), 1752–1179.
12. Gao, S., Suonan, J., Song, G., et al. (2011). A new pilot protection principle for HVDC transmission lines based on current fault component. *Automation of Electric Power Systems*, 35(5), 52–56.
13. Yang, S., Xiang, W and Wen J.(2019). Review of DC fault protection methods for the MMC based DC grid. *Proceedings of the CSEE*. 1–17. <http://kns.cnki.net/kcms/detail/11.2107.TM.20190822.1040.002>.
14. Li, B., Qiu, H., Hong, C., et al. (2018). High-speed direction protection of flexible DC system based on voltage source converter. *Electric Power Automation Equipment*, 38(02), 1–8 (10).2719–2725.
15. Wang, Y., Fu, Y., Zeng, Q., et al. (2019). Review on key techniques for fault protection of flexible DC grids. *High Voltage Engineering*, 45(08), 2362–2374.
16. Jin, X., Song, G., Xu, H., et al. (2014). A novel pilot protection for VSC-HVDC transmission lines using modulus model identification. *Automation of Electric Power Systems*, 38(10), 100–106.
17. Li, M., Jia, K., Bi, T., et al. (2016). Fault distance estimation based protection for DC distribution networks. *Power System Technology*, 40(3), 719–724.
18. Song, G., Wang, T., Zhang, C., et al. (2019). DC line fault identification based on characteristic signal injection using the MMC of sound pole. *Transactions of China Electrotechnical Society*, 34(05), 994–1003.
19. Song, G., Wang, T., Zhang, C., et al. (2019). Adaptive auto-reclosing of DC line based on characteristic signal injection with FB-MMC. *Power System Technology*, 43(01), 149–156.
20. Zhou, M., Xiang, W., Zuo, W., et al.(2019). DC voltage target predetermined control of hybrid MMC to handle DC line fault of overhead DC grid. *Proceedings of the CSEE*, 39(17).5015–5024+5283.
21. Zhou, M., Xiang, W., Zuo, W., et al.(2019). Research on DC fault isolation of MMC based DC grid using the active current-limiting approach. *Proceedings of the CSEE*. 1-14.<http://kns.cnki.net/kcms/detail/11.2107.TM.20190606.1702.006.html>.
22. Zheng, J., Wen, M., Qin, Y., et al.(2018). A novel differential protection scheme with fault line selection capability for HVDC transmission line. *Proceedings of the CSEE*, 38(15) 4350-4358+4635.
23. Spearman, C. (1987). The proof and measurement of association between two things. *The American Journal of Psychology*, 100(3), 441–471.
24. Lee-Rodgers, J., & Nicewander, W. A. (1988). Thirteen ways to look at the correlation coefficient. *The American Statistician*, 42(1), 59–66.

Submit your manuscript to a SpringerOpen[®] journal and benefit from:

- Convenient online submission
- Rigorous peer review
- Open access: articles freely available online
- High visibility within the field
- Retaining the copyright to your article

Submit your next manuscript at ► [springeropen.com](https://www.springeropen.com)
